Hydrothermal Growth and Optical Properties of Doughnut-Shaped ZnO Microparticles

Jianbo Liang, Jianwei Liu, Qin Xie, Sha Bai, Weichao Yu, and Yitai Qian*

Hefei National Laboratory for Physical Sciences at Microscale, Department of Chemistry, University of Science & Technology of China, Hefei, Anhui, 230026, P. R. China

Received: January 27, 2005; In Final Form: March 20, 2005

Doughnut-shaped ZnO microparticles have been grown through a hydrothermal reaction in citrate solution at 120 °C. FESEM reveals that these microparticles consist of regular arranged nanoplates, and there is a concave on the surface of each microparticle. The existence of citrate is vital to the formation of the complex microparticles. Room temperature photoluminescence measurements show strong UV band emission. The yellow and green emissions related to the structure defects can be barely observed, indicating the high crystalline perfection of these microparticles.

Introduction

The shape, crystalline structure, and size of semiconductors are important elements in determining their physical and chemical properties;[1] thus, rational control over these elements has become a hot topic in recent material research fields.[2] ZnO is a unique electronic and photonic semiconductor with band gap of 3.37 eV. Since Yang observed the room temperature UV-lasing from ZnO nanorod arrays,[3] much effort has been devoted to tailor the morphology and size to optimize the optical properties. Thermal evaporation,[4] chemical vapor deposition (CVD),[5] electrodeposition,[6] and template-directed growth[7] are the general technologies. Various ZnO nanostructures such as nanobelts,[4a] nanocombs,[4b] nanosprings, nanohelix,[4c] mesoporous polyhedrals,[4d] hierarchial nanostructures,[5] nanobridges and nanonails,[8] and nanocables[9] have been prepared by these physical methods. Besides, wet chemical methods, which are appealing for their simple manipulation and potential for scale-up, have been applied to synthesize ZnO materials in nano- or microscale. ZnO-oriented helical columns,[10] "corn on the cob" microstructures,[11] flower-like assembles,[12] rotor-like microcrystals,[13] spindle-like rods composed of ring-like nanosheets,[14] hexagonal disks and rings,[15] dandelion-like hollow microspheres,[16] cupped-end microrod bundles,[17] and so on have been synthesized in aqueous solution. Herein, we report a hydrothermal method to synthesize ZnO microparticles, in which citrate salts have been introduced to control over the precipitate procedure. Doughnut-shaped microparticles assembled with well-defined plate-like nanoparticles have been obtained by this method. Moreover, our products show enhanced ultraviolet emission at room temperature, which may inspirit the exploration more convenient access to ZnO materials with unique optical properties.

Experimental Section

All the reagents used in the experiments were in analytical grade (purchased from Shanghai Chemical Industrial Co.) and used without further purification.

To prepare the doughnut-shaped ZnO particles, 2.5 mmol of Zn $(Ac)_2 \cdot 2H_2O$ and 1.75 mmol of citrate potassium were dissolved in 50 mL of distilled water, and then 1.0 mL of 28 wt % commercial ammonia was dripped under constant stirring. The final concentration of the raw materials in solution is zinc, 50 mM; citrate, 37.5 mM; ammonia, 1.06 M. The pH value of the final solution was measured to be 8.7. The mixtures were transferred into a 55 mL Teflon-lined autoclave, maintained at 120 °C for 8 h. The white powders collected from the bottom of the container were washed with distilled water and absolute alcohol in turns, vacuum-dried, and kept for further characterization.

The phase and purity of the products were determined by powder X-ray diffraction (XRD), using a Rigaku (Japan) D/max-γA X-ray diffraction meter equipped with graphite monochromatized Cu Kα radiation ($\lambda = 1.541\,874$ Å). The morphologies and sizes of the samples were examined by field emission scanning electron microscopy (FESEM, JEOL JSM-6700F, operated at 10 kV). The structures of the products were investigated by transmission electron microscopy (Hitachi H-800 with an accelerating voltage of 200 kV). The Raman spectrum was obtained on the JY LABRAM-HR laser micro-Raman spectrometer with 515 emission lines. The room temperature photoluminescence (PL) measurements were also carried out on the micro-Raman spectrometer using the 325 nm excition line of the He−Cd laser. The absorption spectrum was recorded on a UV−vis spectrophotometer (Shimadzu UV-240) in the wavelength range of 340−400 nm.

Results and Discussion

Structure and Morphology. Figure 1 shows the X-ray diffraction (XRD) pattern of the as-prepared products. All the reflection peaks of the products can be indexed as pure hexagonal ZnO with cell parameters $a = 3.249$ Å and $c = 5.206$ Å, which are in good agreement with the literature values (JCPDS card number 36-1451). However, the relative intensity of the peaks corresponding to the (002)/(100) and (002)/(101) planes varied significantly from the literature values, which indicates the different tropism of the products.

The morphology and size of the products were further examined by FESEM. Figure 2a shows that the products consist of relatively uniform doughnut-shaped microparticles with average size of 2.5 μm. It is interesting that there is a concave on one surface of each microparticle, while the opposite side is

* To whom correspondence should be addressed: Fax +86-551-3607402; e-mail ytqian@ustc.edu.cn.

10.1021/jp050485j CCC: $30.25
Published on Web 04/20/2005

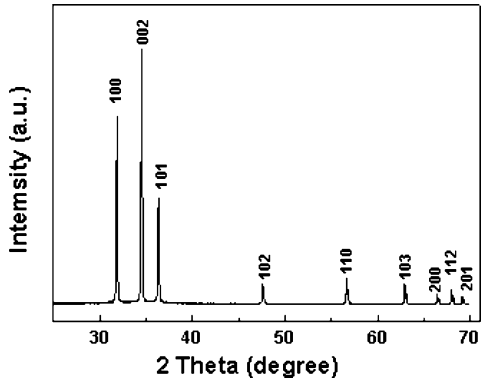

Figure 1. XRD pattern of ZnO powders obtained at 120 °C.

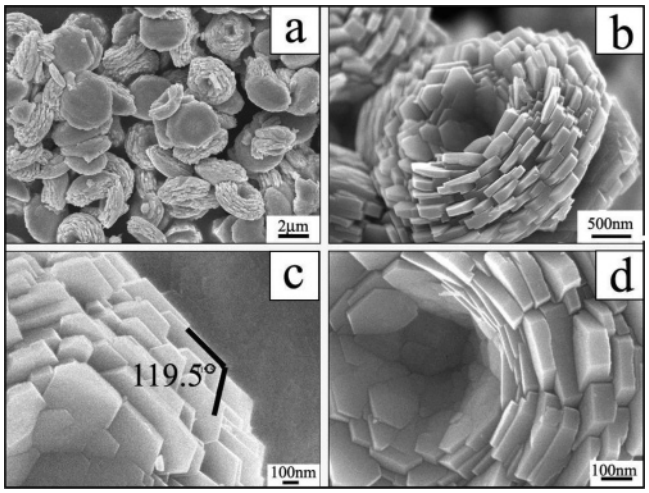

Figure 2. FESEM images of the ZnO powders obtained at 120 °C: (a) low-magnification image; (b) a typical doughnut-shaped microparticle; (c) high-magnification image of the subunits; (d) the central part of the microparticles.

relatively flat. These microparticles are composed of densely packed layers of well-edged nanoplates. The complex microstructures are sufficiently stable that they could not be broken into discrete nanoplates even after long-time ultrasonication. Figure 2b reveals that these nanoplates are arranged at progressively increasing angles to the radial axis and highly directed to form arrays in a regular fashion. The thicknesses of these nanoplates are in the range of 50−70 nm. The detailed information on the nanoplates can be obtained in Figure 2c,d. The nanoplates show well-resolved edges and corners and the surfaces are smooth. The angle between the two adjacent edges of an individual plate is measured to be 119.5°. The corresponding ED pattern recorded from a nanoplate can be indexed to hexagonal ZnO viewed from the [0001] direction, indicating the nanoplate is in a single-crystal structure with (0001) top/bottom surfaces and {10−10} side surfaces (see Supporting Information).

Effect of Reaction Conditions on Growth of ZnO. A serials of experiments showed that the existence of citrate ions played a key role in the formation of the ZnO complex nanostructures. For the controlled experiment in the absence of citrate, the solution became turbid soon when the temperature reached 60 °C, and the products were mainly spherical particles with irregular edges. If citrate were introduced into the solution, the period for the formation of ZnO nuclei (induction and latent periods in the crystal growth process) were remarkably prolonged. These observations suggest that citrate can slow down the nucleation and subsequent crystal growth of ZnO particles.

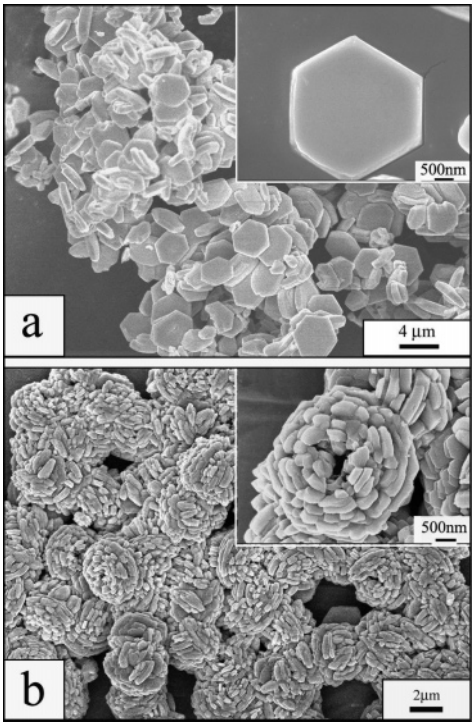

Figure 3. FESEM images of the ZnO microparticles prepared in the presence different amounts of citrate: (a) the hexagonal microplates grown in 50 mM citrate solution; (b) the microspheres grown in 20 mM citrate solution.

In addition, the doughnut-shaped microparticles can be obtained in the presence of either citrate potassium or citrate sodium yet cannot be obtained in the presence of KCl or NaCl solely. This indicates that the citrate anions are responsible for the formation of the complex structures. Moreover, the morphologies of the products varied remarkably when the concentration of citrate changed. If the concentration of citrate increases to 50 mM, all the products comprise of microplates with average size of 2.4 μm (shown in Figure 3a). The surfaces of these plates are rather smooth even though the aging period elongates to 48 h. As the citrate concentration reduces to 20 mM, microspheres with average diameter of 2.6 μm can be obtained (shown in Figure 3b). These microspheres are also composed of plate-like nanoparticles, and some microparticles may have hollow interiors (shown in Figure 3b, inset). It is worth mentioning that these microparticles grown in the presence of different amounts of citrate salts are similar in average size (2.6−2.3 μm in diameter), which suggests that the citrate salts introduced to the solution are good shape modifier but have little effect on the size control of microparticles.

Citrate is an important biological ligand for metal ions. It can forms strong complexes with Ca^{2+}, Mg^{2+}, Fe^{3+}, Zn^{2+}, and Ag^{+} ions.[18] In previous works, citrate have been most widely used as reductant and capping agent in synthesis of elemental Ag, Au, and Ag−Au alloy nanoparticles.[19] It can also serve as shape controllor and stabilizer in the synthesis of $Ni(OH)_2$,[20] calcite,[21] and coated CdSe colloids.[22] On the basis of our experiment results, we believe citrate have two major effects on the growth of the ZnO complex nanostructures. First, as in many surfactant-assisted or ligand-mediated synthesis of shape-controlled materials,[23] citrate molecules may served as surface modifiers, presumably bound to the Zn^{2+} on the polar (0001) planes.[10] ZnO is a polar crystal, which can be described as a number of tetrahedrally coordinated O^{2-} and Zn^{2+} ions stacking alternatively along the *c* axis. Under hydrothermal conditions,

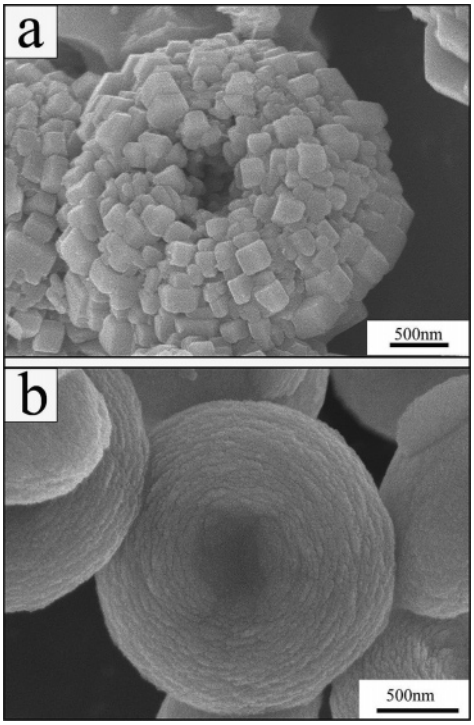

Figure 4. ZnO microparticles obtained at different aging temperatures. (a) Microparticles aging temperature 180 °C; these nanoparticles stacked loosely. (b) Microparticles aging at 95 °C; these nanoparticles packed tightly.

ZnO prefer to grow along the *c* axis to form needle-like microparticles for the specific crystalline structure.[24] In citrate solution, citrate ions may bond to the Zn^{2+} (0001) surfaces through the $-COO^-$ and $-OH$ functions. This surface interaction can inhibit ZnO crystals elongated perpendicular to these planes. In this case, citrate ions may take a similar role as that of the AOT molecules during the formation ZnO hexagonal disks and rings,[15] and this effect is much prominent at higher citrate concentration. Second, citrate can coordinate with zinc ions and control the precipitation process. In our synthesis, we found that the combinations of Zn^{2+} with OH^- could be postponed in citrate solution. The relatively slow reaction is favorable for separating the growth step from the nucleation step and responsible for the narrow size distribution.[23c] Moreover, we found the ZnO powders obtained from the citrate solution possessed highly perfect crystalline structures, as examined by the PL spectrum discussed below. This highly crystalline perfection may also result from the complexation effects of citrate. Citrate can also serve as a transport carrier that mediates the growth of ZnO. Zinc species can be transported to the proper crystalline lattice by citrate ions. It allows the units growth take place on the favorable sites and thus benefits the formation of highly defect-free crystals.

Other conditions such as aging temperature and the amount of ammonia are also important factors to affect the morphologies of the microparticles. For the microparticles grown at 180 °C, the subunits tend to evolve into cube shapes although the microparticles remain the spherical frame (Figure 4a). We find it does not favor the well-regulated stacking fashion at high temperature. However, if the reaction proceeds at lower aging temperature, the size of the subunits can be greatly reduced while the size of these microparticles can be barely changed. Figure 4b is the typical image of the samples prepared at 95 °C, in which these microparticles take a rather circular frame. The sizes of the subunit nanoparticles have sharply decreased to 20−30 nm, and these nanoparticles pack rather densely. It is noted that the superstructured ZnO microparticles grew under an optimized amount of ammonia. In our experiments, the doughnut-shaped microparticles can only be obtained when 0.8−1.2 mL of 28 wt % commercial ammonia were dripped in to the solution.

Studies on the Growth Process. The growth process was also monitored by time-dependent observations. Figure 5a−c shows the combination of TEM and SEM images of the products that were obtained after aging for 0.5, 1.5, and 2 h. Figure 5a reveals that amorphous nanoplates formed at the initial stage. When the aging times extended to 1.5 h, these nanoparticles gradually grew into microdisks, as shown in Figure 5b,c. The corresponding ED pattern recorded from the edge of a microdisk show discrete light sports, conforming the disk is in single-crystal structure. However, the SEM image of the same sample shows that some fine step edges gradually stick out from one surface of the microdisk and lead to the formation of concave in the center. These pictures suggest the formation of the subunits on one surface of the microdisk. Further prolong the aging time to 2 h mainly affected the size of the subunits while the shape of the microparticles were still preserved. As can be observed from Figure 5d, some "sawtooth" has formed on the edge of the microparticle, and the hexagonal frame can still be distinguished. The subsequent growth, which occurred principally around the surface of the primary microdisks, gave rise to the micrometer-sized doughnut-shaped complex crystals, as shown in Figure 2. The main growth process is depicted in Figure 6.

The exact mechanism for the formation of these complex structured ZnO microparticles is still unclear. However, it is obvious that the formation of the textured microplates is of great importance in the growth of the doughnut-shaped microparticles. We noted that the obtained ZnO powders can sedimentate in distilled water rapidly. Thus, to further understand the growth process, we performed the growth of ZnO powders in a biphasic system, in which chlorobenzene was added to the raw solution as oil phase. This designed synthesis experiment is similar to the method that growth of PbS nanorods via a biphasic solvothermal reaction.[25] Chlorobenzene is insoluble in water and inert in the reaction of Zn^{2+} and OH^-. Thus, two layers with an interface will form when they are mixed. The up layer is the aqueous phase containing Zn^{2+}, citrate, and ammonia. The bottom layer is chlorobenzene due to the relatively large density ($\rho = 1.106$ g cm^{-3} at 20 °C). ZnO microparticles formed at the top aqueous solution will sedimentate to the bottom oil phase, and the succeeding epitaxy growth will be held. The morphology of the ZnO powders obtained from the biphasic system after aging for 8 h is presented in Figure 7. The products consist of textured microplates entirely. The well-edged nanoplates can be clearly observed in one surface of the microplate. These observations can further reveal the formation of the textured microplates in the growth of the doughnut-shaped microparticles. The detailed mechanism for the formation of these complex structured ZnO microparticles is still under investigation.

Optical Properties Measurement. ZnO is a wide-band-gap semiconductor ($E_g = 3.37$ eV) with a large exciton binding energy (60 meV). We performed serious optical studies to evaluate the potentially optical qualities of the doughnut-shaped microparticles. The ZnO powders grown according to the Experimental Section were ultrasonic dispersed in diluted water and stored in a quartz cell for UV−vis absorption measurament. The UV−vis spectrum (Figure 8) shows a single absorption peak centered at 368 nm. The calculated band gap is 3.37 eV under current measured conditions, which is in accordance with

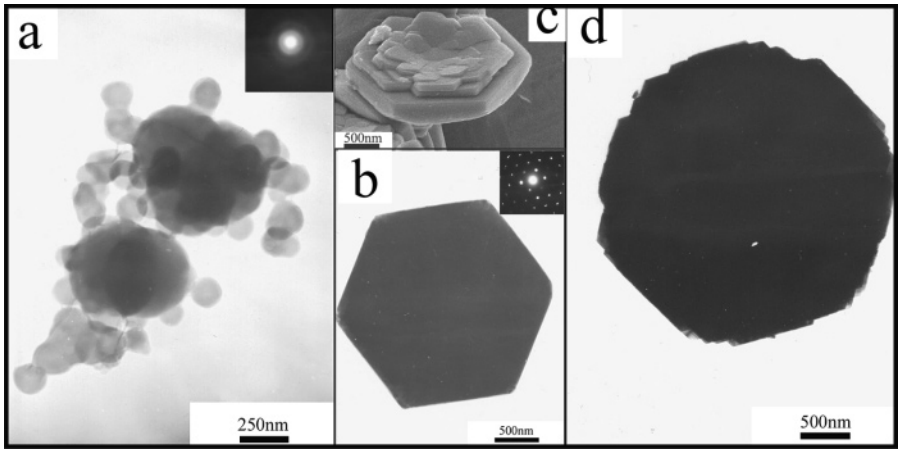

Figure 5. TEM and FESEM image of the samples obtained at different aging period: (a) amorphous nanoplates obtained in 0.5 h; (b, c) textured hexagonal microplate were obtained in 1.5 h; (d) TEM image of the microparticle after aging for 2 h.

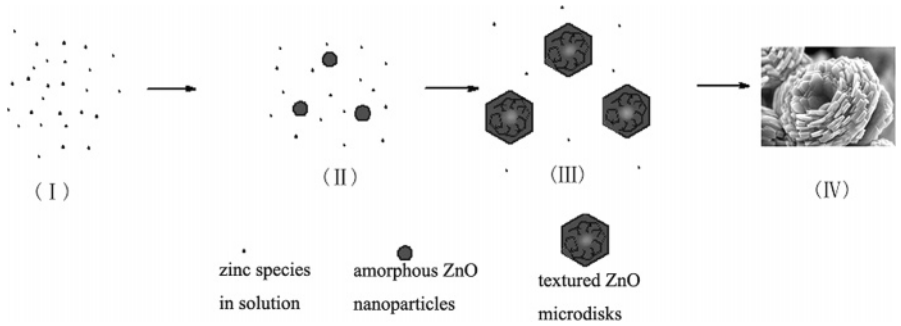

Figure 6. Schematic illustration of the formation process of the ZnO microparticles: (I) zinc citrate solution formed before the aging; (II) formation and growth of tiny ZnO nanoparticles with poor crystallization; (III) the shape evolution of textured ZnO disks; (IV) the final complex structured ZnO microparticles.

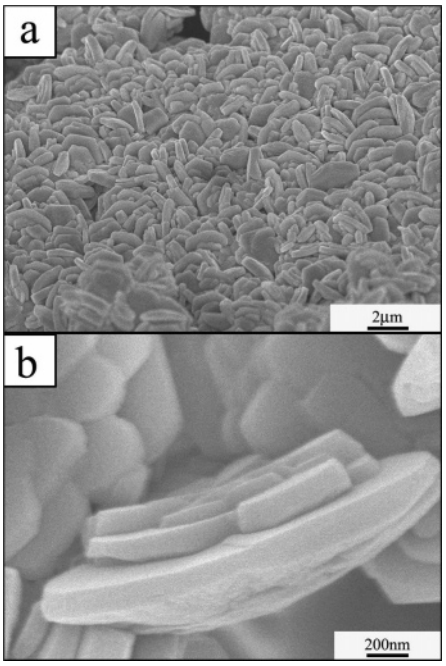

Figure 7. FESEM images of the ZnO microparticles obtained in the designed system after aging at 120 °C for 8 h. The products consist of textured ZnO microdisks.

the bulk values. No quantum confinement effects were observed because of the relatively large size. The Raman spectrum (see Supporting Information) measured at room temperature show three peaks. The peak of Raman shifts of 437 cm^{-1} is the ZnO nonpolar optical phonons (E_2). The peak at 581 cm^{-1} is attributed to the longitudinal optical (LO) modes, and the

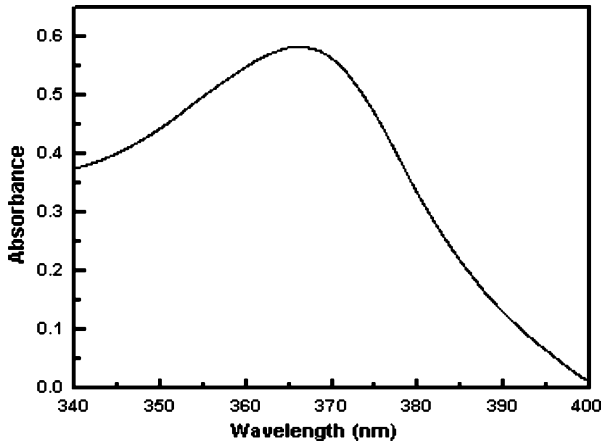

Figure 8. UV−vis absorption spectrum of the doughnut-shaped ZnO microparticles. The single absorption peak located at 368 nm.

second-order modes are located 332 cm^{-1}. All of the Raman peaks from the ZnO powders agree well with the published data.[26]

We further carried out room temperature photoluminescence measurement to examine the quality of the products. As shown in Figure 9, the spectrum of the products obtained at 120 °C (curve a) shows the UV emission band centered at 385 nm with a half-maximum width of 21 nm. At room temperature, ZnO typically exhibits UV band edge emission and broad visible emissions at green and yellow bands. The UV band edge emission is attributed to free excitonic emission. For the green and yellow emissions, it has been generally believed that these visible emissions are due to transition in defect states, in particular the oxygen vacancies.[25,26] Thus, the quality of ZnO

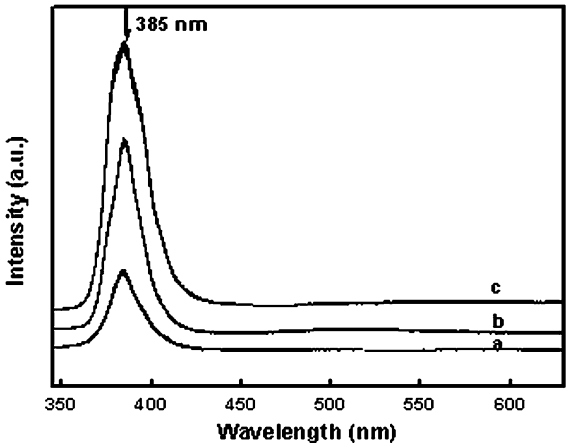

Figure 9. Room temperature photoluminescence spectra of ZnO powders grown at different temperatures: (a) 120, (b) 160, and (c) 180 °C.

can be evaluated from the intensity ratio of the two emission peaks. For the doughnut-shaped ZnO powders obtained in citrate solution, the green and yellow emissions originating from the structure defects can barely be observed. Moreover, the UV emission can be further enhanced with elevated growth temperature, as indicated in curves b and c. The enhanced UV emission indicates that the microparticles possess high crystalline perfection. We have attributed the high crystalline quality to the complexation effects of citrate. Citrate can control release of Zn^{2+} during the growth of ZnO crystals. It benefits the growth units to take the proper growth sites, thus favoring the formation of highly defect-free crystals.

In summary, doughnut-shaped ZnO nanostructures have been synthesized under hydrothermal conditions. Citrate salts have been introduced as shape modifier and proved to be efficient to control the shape of the ZnO nanostructures. The effects of the aging temperature and the amount of commercial ammonia have been discussed. The products show a strong UV band emission centered at 385 nm. The synthesis route is easily controllable and well reproducible and may be feasible to develop into scale-up production.

Acknowledgment. Financial support from the National Nature Science Fund of China and the 973 Project of China is appreciated.

Supporting Information Available: FESEM images of the flat side and the TEM images and the ED pattern of the microparticles (Figures a and b, respectively); Raman spectrum of the ZnO powders (Figure c). This material is available free of charge via the Internet at http://pubs.acs.org.

References and Notes

(1) (a) Lieber, C. M. *Solid State Commun.* **1998**, *107*, 607. (b) Alivisatos, A. P. *Science* **1996**, *271*, 933.

(2) Xia, Y.; Yang, P.; Sun, Y.; Wu, Y.; Mayer, B.; Gates, B.; Yin, Y.; Kim, F.; Yan, H. *Adv. Mater.* **2003**, *15*, 353.

(3) Huang, M. H.; Mao, S.; Feick, H.; Yan, H. Q.; Wu, Y. Y.; Kind, H.; Weber, E.; Russo, R.; Yang, P. D. *Science* **2001**, *292*, 1897.

(4) (a) Pan, Z. W.; Dai, Z. R.; Wang, Z. L. *Science* **2001**, *291*, 1947. (b) Wang, Z. L.; Kong, X. Y.; Zuo, J. M. *Phys. Rev. Lett.* **2003**, *91*, 185502. (c) Kong, X. Y.; Wang, Z. L. *Nano Lett.* **2003**, *3*, 1265. (d) Gao, P. X.; Wang, Z. L. *J. Am. Chem. Soc.* **2003**, *125*, 11299.

(5) Lao, J. Y.; Wen, J. G.; Ren, Z. F. *Nano Lett.* **2002**, *2*, 1287.

(6) Choi, K. S.; Lichtenegger, H. C.; Stucky, G. D. *J. Am. Chem. Soc.* **2002**, *124*, 12402.

(7) Liu, C. H.; Zapien, J. A.; Yao, Y.; Meng, X. M.; Lee, C. S.; Fan, S. S.; Lifshitz, Y.; Lee, S. T. *Adv. Mater.* **2003**, *15*, 838.

(8) Lao, J. Y.; Huang, J. Y.; Wang, D. Z.; Ren, Z. F. *Nano Lett.* **2003**, *3*, 235.

(9) Wu, J. J.; Liu, S. C.; Wu, C. T.; Chen, K. H.; Chen, L. C. *Appl. Phys. Lett.* **2002**, *81*, 1312.

(10) (a) Tian, Z. R.; Voigt, J. A.; Liu, J.; Mckenzie, B.; Mcdermott, M. J. *J. Am. Chem. Soc.* **2002**, *124*, 12954. (b) Tian, Z. R.; Voigt, J. A.; Liu, J.; McKenzie, B.; McDermott, M. J.; Rodriguez, M. A.; Konishi, H. Xu, H. F. *Nat. Mater.* **2003**, *2*, 821.

(11) Taubert, A.; Kubel, C.; Martin, D. C. *J. Phys. Chem. B* **2003**, *107*, 2660.

(12) Zhang, H.; Yang, D.; Ji, Y.; Ma, X.; Xu, J.; Que, D. *J. Phys. Chem. B* **2004**, *108*, 3955.

(13) Gao, X. P.; Zheng, Z. F.; Zhu, H. Y.; Pan, G. L.; Bao, J. L.; Wu, F.; Song, D. Y. *Chem. Comm.* **2004**, *12*, 1428.

(14) Liu, B.; Yu, S. H.; Zhang, F.; Li, L. J.; Zhang, Q.; Ren, L.; Jiang, K. *J. Phys. Chem. B* **2004**, *108*, 4338.

(15) Li, F.; Ding, Y.; Gao, P. X.; Xin, X. Q.; Wang, Z. L. *Angew. Chem., Int. Ed.* **2004**, *43*, 5238.

(16) Liu, B.; Zeng, H. C. *J. Am. Chem. Soc.* **2004**, *126*, 16744.

(17) Jiang, C. L.; Zhang, W. Q.; Zou, G. F.; Yu, W. C.; Qian, Y. T. *J. Phys. Chem.* **2005**, *109*, 1361.

(18) Parkinson, J. A.; Sun, H. Z.; Sadler, P. J. *Chem. Commun.* **1998**, *8*, 881.

(19) (a) Pillai, Z. S.; Kamat, P. V. *J. Phys. Chem. B* **2004**, *108*, 945. (b) Brown, K. R.; Walter, D. G.; Natan, M. J. *Chem. Mater.* **2000**, *12*, 306. (c) Mallin, M. P.; Murphy, C. J. *Nano Lett.* **2002**, *2*, 1235.

(20) Meyer, M.; Bée, A.; Talbot, D.; Cabuil, V.; Boyer, J. M.; Répetti, B.; Garrigos, R. *J. Colloid Interface Sci.* **2004**, *277*, 309.

(21) Meldruma, F. C.; Hyde, S. T. *J. Cryst. Growth* **2001**, *231*, 544.

(22) Wang, Y.; Tang, Z. Y.; Correa-Duarte, M. A.; Pastoriza-Santos, I.; Giersig, M.; Kotov, N. A.; Liz-Marzan, L. M. *J. Phys. Chem. B* **2004**, *108*, 15461.

(23) See examples: (a) Peng, X. G. *Adv. Mater.* **2003**, *15*, 459. (b) Sun, Y.; Yin, Y.; Mayer, B.; Herricks, T.; Xia, Y. *Chem. Mater.* **2002**, *14*, 4736. (c) Liu, Z. P.; Li, S.; Yang, Y.; Peng, S.; Hu, Z. K.; Qian, Y. T. *Adv. Mater.* **2003**, *15*, 1946.

(24) Li, W. J.; Shi, E. W.; Zhong, W. Z.; Yin, Z. W. *J. Cryst. Growth* **1999**, *203*, 186.

(25) Mo, M. S.; Shao, M. W.; Hu, H. M.; Yang, L.; Yu, W. C.; Qian, Y. T *J. Cryst. Growth* **2002**, *244*, 364.

(26) (a) Damen, T. C.; Porto, S. P. S.; Tell, B. *Phys. Rev.* **1966**, *142*, 570. (b) Arguello, C. A.; Rousseau, D. L.; Porto, S. P. S. *Phys. Rev.* **1969**, *181*, 1351.

(27) Vanheusden, K.; Warren, W. L.; Seager, C. H.; Tallant, D. R.; Voigt, J. A.; Gnade, B. E. *J. Appl. Phys.* **1996**, *79*, 7983.

(28) Li, D.; Leung, Y. H.; Djurišiæ, A. B.; Liu, Z. T.; Xie, M. H.; Shi, S. L.; Xu, S. J.; Chan, W. K. *Appl. Phys. Lett.* **2004**, *85*, 1601.